








RESEARCH ARTICLE

Skeletal and muscular pelvic morphology of hillstream loaches (Cypriniformes: Balitoridae)

Callie H. Crawford¹  | Zachary S. Randall²  | Pamela B. Hart³  |
 Lawrence M. Page²  | Prosanta Chakrabarty³  | Apinun Suvarnaraksha⁴  |
 Brooke E. Flammang¹ 

¹Department of Biological Sciences, New Jersey Institute of Technology, Newark, New Jersey

²Florida Museum of Natural History, University of Florida, Gainesville, Florida

³Museum of Natural Science, Louisiana State University, Baton Rouge, Louisiana

⁴Faculty of Fisheries Technology and Aquatic Resources, Maejo University, Chiang Mai, Thailand

Correspondence

Callie H. Crawford, Department of Biological Sciences, New Jersey Institute of Technology, Newark, New Jersey, 07102, USA.
 Email: chc24@njit.edu

Funding information

American Museum of Natural History (Lerner-Gray Grant for Marine Research); American Society of Ichthyologists and Herpetologists (Raney Fund Award); Duke University (Research Triangle Nanotechnology Network Free-Use); National Science Foundation, Grant/Award Number: 1839915; Sigma Xi (Grants in Aid of Research)

Abstract

The rheophilic hillstream loaches (Balitoridae) of South and Southeast Asia possess a range of pelvic girdle morphologies, which may be attributed to adaptations for locomotion against rapidly flowing water. Specifically, the connectivity of the pelvic plate (basipterygium) to the vertebral column via a sacral rib, and the relative size and shape of the sacral rib, fall within a spectrum of three discrete morphotypes: long, narrow rib that meets the basipterygium; thicker, slightly curved rib meeting the basipterygium; and robust crested rib interlocking with the basipterygium. Species in this third category with more robust sacral rib connections between the basipterygium and vertebral column are capable of walking out of water with a tetrapod-like lateral-sequence, diagonal-couplet gait. This behavior has not been observed in species lacking direct skeletal connection between the vertebrae and the pelvis. The phylogenetic positions of the morphotypes were visualized by matching the morphological features onto a novel hypothesis of relationships for the family Balitoridae. The morphotypes determined through skeletal morphology were correlated with patterns observed in the pelvic muscle morphology of these fishes. Transitions towards increasingly robust pelvic girdle attachment were coincident with a more anterior origin on the basipterygium and more lateral insertion of the muscles on the fin rays, along with a reduction of the superficial abductors and adductors with more posterior insertions. These modifications are expected to provide a mechanical advantage for generating force against the ground. Inclusion of the enigmatic cave-adapted balitorid *Cryptотора thamicola* into the most data-rich balitorid phylogeny reveals its closest relatives, providing insight into the origin of the skeletal connection between the axial skeleton and basipterygium.

KEYWORDS

computed tomography, fish, musculature, pelvic morphology, phylogeny, walking

1 | INTRODUCTION

The hillstream loaches, Balitoridae (Cypriniformes), are a family of 101 species of morphologically diverse rheophilic freshwater fishes

inhabiting south and southeast Asia (Fricke, Eschmeyer, & van der Laan, 2019; Kottelat, 2012; Nelson, Grande, & Wilson, 2016). Species in this family are characterized by a dorsoventrally flattened body, enlarged pelvic basipterygium, and expanded pectoral and pelvic fins

that are ventrally located (Figure 1; de Meyer & Geerinckx, 2014; Hora, 1932; Nelson et al., 2016). In the majority of extant teleost fishes, the pelvic fins are positioned abdominally in earlier diverging groups, with more recent lineages having the fins located more anteriorly and attached to the pectoral girdle (Yamanoue, Setiamarga, & Matsuura, 2010). In the balitorids, there is a skeletal connection between the pelvic plate (basipterygium) and the vertebral column via a modified rib and its distal ligament (Chang, 1945; Sawada, 1982; Saxena & Chandy, 1966).

The morphology of these loaches may be an adaptation for life in their fast-flowing environment. The hypertrophied ossification observed in the modified pleural rib, referred to here as a sacral rib, is likely an adaptation that allows the fish to transmit counterforces against the substrate to hold against the flow of fast moving water (Ahlberg, 2019; Chang, 1945). The hyperossification and connection between the basipterygium and axial skeleton in these fishes is reminiscent of the sacrum in terrestrial tetrapods (Flammang, Suvarnaksha, Markiewicz, & Soares, 2016). This structural connection between the axial and appendicular skeleton in tetrapods was important for the evolution of terrestrial walking (Lebedev, 1997). The dorsoventral body compression seen in these fishes, along with the horizontal placement of their broad pelvic and pectoral fins, allows for increased contact with the substrate to support station-holding in fast water (Chang, 1945; Lujan & Conway, 2015; Sawada, 1982). Adhesive pads are also present on the leading pectoral and pelvic fin rays formed from thickened subepidermal connective tissue on the ventral side of the fin, and possess keratinized uncili (Chang, 1945; Conway, Lujan, Lundberg, Mayden, & Siegel, 2012; Hora, 1930; Sawada, 1982; Saxena & Chandy, 1966). Such pads have been recorded in taxa of four rheophilic Ostariophysi orders (Gonorynchiformes, Cypriniformes, Characiformes, and Siluriformes; Conway et al., 2012).

Recently, the cave-obligate balitorid loach, *Cryptotora thamicola*, was shown to walk with a salamander-like lateral-sequence diagonal-couplets (LSDC) gait (Flammang et al., 2016). The walking behavior

recorded in *C. thamicola* is facilitated by morphological features converging on terrestrial tetrapod synapomorphies, including robust pectoral and pelvic girdles, a connection of the pelvic girdle to the vertebral column via a fused sacral rib, broad neural spines, and zygopophyses connecting serial vertebrae. We hypothesize that the features supporting terrestrial locomotion are also features that support life in fast moving water and are present to varying degrees throughout Balitoridae.

Previous study separating balitorids and their sister family Gastromyzontidae based on morphology has led to the characterization of morphotypes based on the number of simple pelvic radials (Hora, 1930) and basipterygium shape, most notably the presence of lateral foramina (Balitoridae) or posterolateral horns (Gastromyzontidae) as the point of connection between the sacral rib and the pelvic plate (Sawada, 1982). Herein, we describe the skeletal and muscular pelvic fin modifications found throughout balitorid loaches and identify three discrete subgroups based on morphological features that are functionally important for walking behavior. In addition, we present here a novel molecular phylogeny that includes *Cryptotora thamicola*, providing a framework for the comparison of these morphotypes from a phylogenomic perspective.

2 | MATERIALS AND METHODS

2.1 | Species and specimens

This study follows Kottelat (2012) and Tan and Armbruster (2018) in the classification of Balitoridae. We used a broad sampling of natural history museum specimens for this study, representing 29 species and 14 of 16 balitorid genera for the skeletal work (Table 1). From the skeletal observations, one species per morphotype was analyzed for muscle morphology. The outgroup comparison for skeletal and muscular morphology was *Carassius auratus* (Cyprinidae). Specimens were

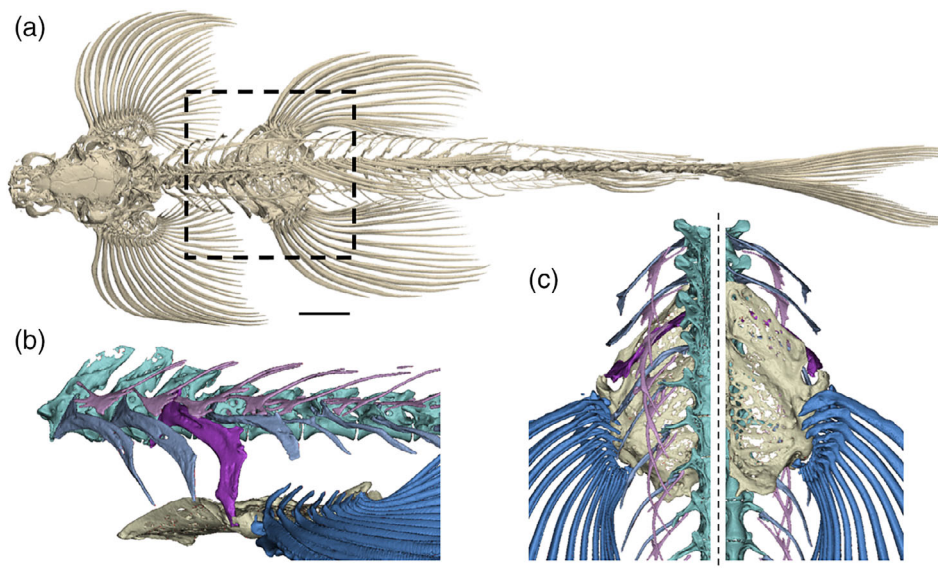


FIGURE 1 *Cryptotora thamicola* (MARNM 6183), anatomical key to study region from a μ CT scan, (a) complete skeleton from the dorsal view, (b) lateral, and (c) dorsal (left) and ventral (right) view of the study region (anterior to top), intermuscular bone (light purple), pelvic radials (dark blue), basipterygium (tan), ribs (light blue), and sacral ribs (dark purple). Scale bars = 2.5 mm

TABLE 1 List of study taxa with associated museum and specimen numbers used in this study with the designated morphotype determined with μ CT scan segmentations

Taxon	Museum/institution	Specimen number	Morphotype
<i>Carassius auratus</i>	Flammang Lab/NJIT	N/A	T
<i>Ghatsa montana</i>	CAS	SU39871	M1
<i>Homaloptera bilineata</i>	USNM	378394	M1
<i>Homaloptera ogilviei</i>	USNM	288431	M1
<i>Homaloptera orthogoniata</i>	Flammang Lab/NJIT	N/A	M1
<i>Homaloptera parclitella</i>	Flammang Lab/NJIT	N/A	M1
<i>Homalopterula vanderbilti</i>	ANSP	68689	M1
<i>Neohomaloptera johorensis</i>	UF	166089	M1
<i>Balitoropsis zollingeri</i>	UF	235547	M2
<i>Hemimyzon formosanus</i>	USNM	161711	M2
<i>Hemimyzon taitungensis</i>	USNM	300711	M2
<i>Homalopteroides nebulosus</i>	UF	1235748	M2
<i>Homalopteroides rupicola</i>	CAS	231726	M2
<i>Homalopterula gymnogaster</i>	USNM	409946	M2
<i>Homalopterula heterolepis</i>	AMNH	9263	M2
<i>Homalopterula ripleyi</i>	USNM	390014	M2
<i>Jinshaia abbreviata</i>	ANSP	185166	M2
<i>Lepturichthys fimbriatus</i>	ANSP	185165	M2
<i>Sinogastromyzon puliensis</i>	UF	185384	M2
<i>Balitora burmanica</i>	USNM	44808	M3
<i>Balitora</i> sp	ANSP	179834	M3
<i>Balitoropsis ophiolepis</i>	UF	166109	M3
<i>Bhavana australis</i>	USNM	165107	M3
<i>Cryptотора thamicola</i>	MARNM	6183	M3
<i>Hemimyzon macroptera</i>	USNM	293925	M3
<i>Homalopteroides smithi</i>	UF	172923	M3
<i>Homalopteroides stephensoni</i>	ZRC	FIS51741	M3
<i>Homalopteroides tweediei</i>	Flammang Lab/NJIT	N/A	M3
<i>Homalopteroides weberi</i>	USNM	393729	M3
<i>Pseudohomaloptera leonardi</i>	UF	183398	M3

Abbreviations: AMNH, American Museum of Natural History; ANSP, Academy of Natural Sciences of Drexel University; CAS, California Academy of Sciences; MARNM, Maejo Aquatic Resources Natural Museum, Maejo University, Nong Han; UF, Florida Museum of Natural History; USNM, Smithsonian Institute; and ZRC, Zoological Reference Collection at the Lee Kong Chian Natural History Museum.

borrowed from the American Museum of Natural History (AMNH), the Academy of Natural Sciences of Drexel University (ANSP), the California Academy of Sciences (CAS), the Florida Museum of Natural History (UF), Maejo Aquatic Resources Natural Museum, Maejo University, Nong Han (MARNM), the Smithsonian National Museum of Natural History (USNM), and the Zoological Reference Collection at the Lee Kong Chian Natural History Museum (ZRC).

2.2 | μ CT scanning, staining, and segmentation

In order to visualize skeletal and muscular morphology, we collected Computed Microtomographic (μ CT) scans of all loaned species and, when permitted by collections staff and curators, stained specimens

in phosphotungstic acid (PTA) to increase radiopacity of muscle. We μ CT-scanned museum specimens (Table 1) using a Bruker SkyScan 1,275 at the New Jersey Institute of Technology Otto York Bio-imaging facility, a Bruker SkyScan 1,275 at Microphotonics (Allentown, PA), a GE Phoenix v|tome|x M at the American Museum of Natural History, GE Phoenix v|tome|x M scanner (GE Measurement & Control, Boston, MA) at the University of Florida's Nanoscale Research Facility, and a Nikon XTH 225 ST at Duke University. The scanner settings varied due to specifications of the different types of scanners and are available in Supporting information, Table S1. Specimens for this study were μ CT-scanned at voxel sizes ranging from 10 to 26 μ m.

After the initial scan for skeletal morphology, specimens were stained in 3% phosphotungstic acid (PTA) solution in 70% ethanol for

2 weeks to allow for full penetration of the stain. Phosphotungstic acid readily stains tissues with high protein and collagen content, including muscles and ligaments; however, it does not stain cartilage (Descamps et al., 2014; Metscher, 2009). Staining with PTA causes considerably less specimen shrinkage than has been seen with iodine staining, (Buytaert, Goyens, De Greef, Aerts, & Dirckx, 2014), which we verified through comparison to original scans, and does not visibly discolor specimens. After staining, we scanned the specimens again at settings appropriate for stained material.

Scan data were reconstructed using software accompanying the different scanners, following manufacturer guidelines for appropriate reconstructions. We then used FIJI (Schindelin et al. 2012) and DataViewer (Bruker, Belgium) to crop datasets for visualization and segmentation in Mimics Segmentation Software Research Suite v20.0 (Materialise, Belgium). The digital dissections segmented from the scans were used to separate the species into morphotypes based on the shape of the sacral rib, its connection to the basiptyrgium, and the shape of the basiptyrgium.

2.3 | Shape analysis

Rib shape of 29 balitorid species and one outgroup (*Carassius auratus*, Cyprinidae) was analyzed using the Elliptical Fourier Descriptors (EFD) approach (Kuhl & Giardina, 1982) in order to analyze 2-dimensional rib shape changes among the three morphotypes. 2D-images were taken of the 3D-segmented models from the right sacral rib of each species in the study. The rib models were oriented perpendicularly to the screen to capture their overall shape. The 2D-images were converted to grayscale bitmaps in Fiji (Schindelin et al., 2012) for outline analysis and converted to chain code using the SHAPE 1.3 program (Iwata & Ukai, 2002). Chain codes along the perimeter of each rib shape were used to create a harmonic series using 80 harmonics within SHAPE 1.3. The principal component analysis (PCA) was completed using PrinComp, another program within the SHAPE 1.3 software. The PC-scores from SHAPE 1.3 were used to visualize the variance within and between the morphotypes. One specimen for each species was included in the shape analyses. To quantitatively test the morphotypes delimited from the shape data of the analyzed species, Linear Discriminant Analysis was run using the *lda* function in the R-package MASS (Ripley & Venables, 2002). The confusion matrix function was employed to compare our classification of morphotype with that predicted from the LDA.

2.4 | Physiological cross-sectional area

Within Mimics Segmentation Software, the μ CT-scan data of the PTA-stained specimens were used for muscle analysis. Fiber lengths were calculated by measuring the length of the fiber bundles and taking the average over 3–10 bundles, with more bundles measured whenever possible. The physiological cross-sectional area (PCSA) of each muscle was calculated as muscle volume/fiber length and then

normalized. The fiber lengths and PCSA were normalized to the total fish volume measured from Mimics using $V^{1/3}$ and $V^{2/3}$, respectively. Normalized PCSAs were plotted against normalized fiber lengths to generate a functional morphospace of the pelvic fin muscles. This morphospace creates a visualization of the trade-offs between muscle force (PCSA) and range of muscle shortening (fiber length; Allen, Eley, Jones, Wright, & Hutchinson, 2010; Dickson & Pierce, 2019; Lieber, 2002). Following Allen et al. (2010), the morphospace can be broken into quadrants with the upper left being “force-specialized” muscles with large forces and small extension ranges; upper right are “powerful” muscles with large forces and extension ranges; lower right muscles are “displacement-specialized” with low force and large extension; and finally the lower left are “generalized” muscles with low force and small extension.

2.5 | Phylogenomics

For our molecular phylogeny, we sampled across seven families of loaches (Cypriniformes) with members of the Vaillantellidae used as the outgroup (Supporting information 2, Table S1, $N = 62$). Samples were chosen due to changing taxonomic classification among the loach families (Kottelat, 2012; Randall & Page, 2015; Šlechtová, Bohlen, & Tan, 2007; Tan & Armbruster, 2018). We used ultra-conserved element (UCE) loci as a reduced representation genomic dataset to reconstruct the evolutionary relationships. These loci have both areas of high conservation, allowing for comparisons across species, and also flanking regions that contain genetic variability to allow for identification of diversity (Faircloth et al., 2012). Our molecular methods and bioinformatics processing were identical to those in Hart et al. (2020; detailed in Supporting information 2). We partitioned the data using Sliding-Window Site Characteristic based on site entropies (Tagliacollo & Lanfear, 2018) in PartitionFinder2 (v.2.1.1; Lanfear, Frandsen, Wright, Senfeld, & Calcott, 2017) on CIPRES Gateway. We reconstructed relationships using Maximum Likelihood (RAxML-HPC2 on XSEDE v.8.2.10; Stamatakis, 2014) and a coalescent species tree method (SVDQuartets in PAUP* v.4.0a; PAUP*: Swofford, 2002; SVDQuartets: Chifman & Kubatko, 2014), both using a concatenated dataset of 75% completeness ($N = 411$ loci). We matched morphotypes from our skeletal morphology portion onto the multispecies coalescent tree to visualize the distribution of morphotypes in a phylogenetic context. Collaboration on this project was preceded by independent studies of morphology and molecular phylogenetics. Due to the nature of the work required for these different approaches (e.g., formalin-fixed specimens can be used for morphological work, but not always for a molecular approach), it was not possible to get permission to stain and scan all species sampled for the phylogeny nor obtain tissue samples from all species scanned.

We tested for phylogenetic signal in our discrete character of morphotypes using the *phylo.signal.disc* function in R,v.4.0 (Bush et al., 2016) following pruning our tree for only species that overlapped in both morphological and molecular datasets. We also pruned the tree to include a single tip (individual) per species so as not to bias

the distribution of morphotypes. Phylogenetic signal is the notion that closely related species resemble each other more so than they resemble randomly chosen species from the phylogeny (Blomberg, Garland, & Ives, 2003; Münkemüller et al., 2012). The *phylo.signal.disc* function uses the Maddison and Slatkin (1991) method, in which the number of minimum observed evolutionary transitions at nodes is compared to the distribution of transitions from a null model. If the observed number is significantly less than the median from the null distribution, a significant *p* value is inferred. We performed 999 randomizations. To examine if our small sample size for M1 ($N = 2$) affected our phylogenetic signal results, we analyzed the data with and without M1 specimens.

3 | RESULTS

3.1 | Skeletal morphology

We found a broad spectrum of pelvic morphology in the balitorids studied here; this variation was separated into three pelvic morphotypes determined from μ CT-reconstructions of the skeletal structures in the pelvic region (Figure 2). The structures we used to distinguish the morphotypes were the enlargement or elongation of the sacral rib, the curvature of the sacral rib, the presence of a flared lateral edge of the sacral rib as previously described in *Cryptoptora thamicola* (Flammang et al., 2016), the extent of the connection to the basipterygium, and the shape of the puboischiadic plate, or basipterygium (puboischiadic plate in Flammang et al., 2016).

3.1.1 | Cyprinid outgroup

In the general teleost outgroup used here for skeletal comparisons, *Carassius auratus* (Figure 2, row 1), the vertebrae lacked zygapophyses or similar bony connections between serial neighbors. Thoracic ribs were long and tapered, attached to the anteroventrally positioned parapophysis and diapophysis, and extended ventrally. Importantly, the ribs did not attach to the basipterygium; the pelvic fin bones hang in a muscular sling in the ventral body, as is considered the more ancestral condition (Yamanoue et al., 2010). The basipterygium is long and narrow, and the two bilateral halves joined only at the anterior symphysis and posteriorly between the fin rays; the central halves of the pelvis did not meet at the midline. There were no lateral foramina in the basipterygium. The posterior processes of the basipterygium were long and narrow and did not connect at the midline but instead tapered caudally and laterally.

3.1.2 | Balitorid Morphotype 1

Of the 29 balitorids scanned for this study, seven fit into Morphotype 1 (M1; Figure 2, Row 2): *Ghatsa montana*, *Homaloptera bilineata*, *Homaloptera ogilviei*, *Homaloptera orthogoniata*, *Homaloptera parclitella*,

Homaloptera vanderbilti, and *Neohomaloptera johorensis* (Table 1). Of the three morphotypes, M1-fishes were the most similar to the typical teleost anatomy. Thoracic ribs were attached to the anteroventrally positioned parapophysis and more dorsally located diapophysis and extend ventrally. The attachment area of the rib to the vertebrae was smallest, and the angle of this attachment was shallowest compared to the other two morphotypes. On the anterodorsal aspect of the thoracic vertebral centra of all species were small bilateral anteriorly facing articular facets, or zygapophyses. Posteriorly facing articular facets were located at the posterior end of the thoracic vertebral centra on all species except for *Homaloptera bilineata* and *Neohomaloptera johorensis*. In M1, the anterior and posterior zygapophyses or the vertebra supporting the sacral rib were significantly smaller than those of M2 and M3, averaging 12.53% ($n = 7$, $SD = 0.06$) and 5.19% ($n = 7$, $SD = 0.03$) of the vertebral length, respectively. Zygapophyses were not observed on caudal vertebrae, that is, those caudal to the sacral vertebra. The intermuscular bones of fishes in morphotype 1 were simple and had low visibility in some μ CT-scans (*Neohomaloptera johorensis*, Figure 2, light purple). One rib, described here as the sacral rib (after Flammang et al., 2016; Figure 2, dark purple) extended distally through the lateral foramen of the basipterygium. The sacral rib in M1 fishes was morphologically similar to the thoracic ribs preceding it, with the exclusion of its proximity to the basipterygium. The basipterygium averaged 72.60% as wide as it was long ($n = 7$, $SD = 0.15$) and was roughly diamond-shaped, with the widest aspect at the anterior attachment of the fin rays. The bilateral halves of the basipterygium were joined at the midline, creating a dome that extended dorsally with a wide ventral concavity; however, the lateral aspects of basipterygium were flat with a large lateral foramen on each side, just anterior to the pelvic fin. The bilateral posterior processes of the basipterygium were thin and tapered toward each other.

3.1.3 | Balitorid Morphotype 2

Morphotype two (M2) exhibited intermediate rib morphology (Table 1; Figure 2, Row 3) and was comprised of 11 of the 29 studied species (*Balitoropsis zollingeri*, *Hemimyzon formosanus*, *Hemimyzon taitungensis*, *Homaloptera ripleyi*, *Homalopteroides nebulosus*, *Homalopteroides rupicola*, *Homaloptera gymnogaster*, *Homaloptera heterolepis*, *Jinshaia abbreviata*, *Lepturichthys fimbriata*, and *Sinogastromyzon puliensis*). Thoracic ribs, including the sacral rib, were attached to vertebral centra with a larger contact area than in M1-fishes: the parapophysis was in the typical anteroventral position but the diapophysis was dorsal and more posterior, approximately mid-centra. The anterior and posterior zygapophyses in M2-fishes were significantly larger than those of M1 and smaller than those in M3, averaging 19.44% ($n = 11$, $SD = 0.05$) and 8.60% ($n = 11$, $SD = 0.03$) of the vertebral length, respectively. The sacral rib was distinguishable from the distally tapered thoracic ribs preceding it by having a broad distal end, which was anchored through the lateral foramen of the basipterygium via a distal ligament. Basipterygium width was 92.67% of its length ($n = 11$, $SD = 0.14$), and the central

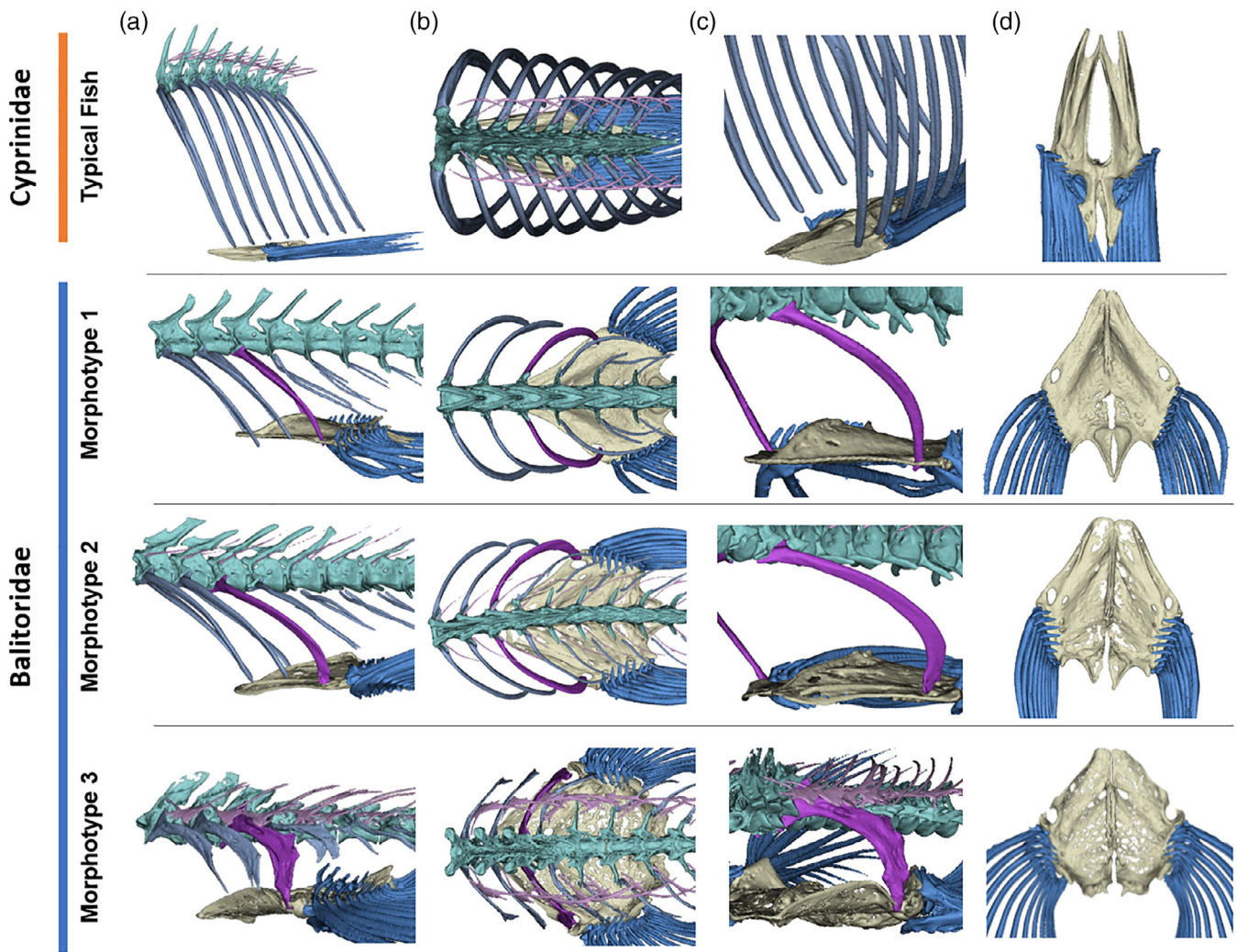


FIGURE 2 Representation of variation in balitorid pelvic morphology shown from (a) lateral view, (b) dorsal view, (c) close-up view of sacral rib with other ribs removed, and (d) dorsal view of the basipterygium and pelvic fin rays. Typical fish morphology, *Carassius auratus* (Flammang Lab); Morphotype 1, *Neohomaloptera johorensis* (UF 166089); Morphotype 2, *Homaloptera vanderbilti* (ANSP 68689); and Morphotype 3, *Cryptotora thamicola* (MARNM 6183). Intermuscular bone (light purple), pelvic radials (dark blue), basipterygium (tan), ribs (light blue), and sacral ribs (dark purple)

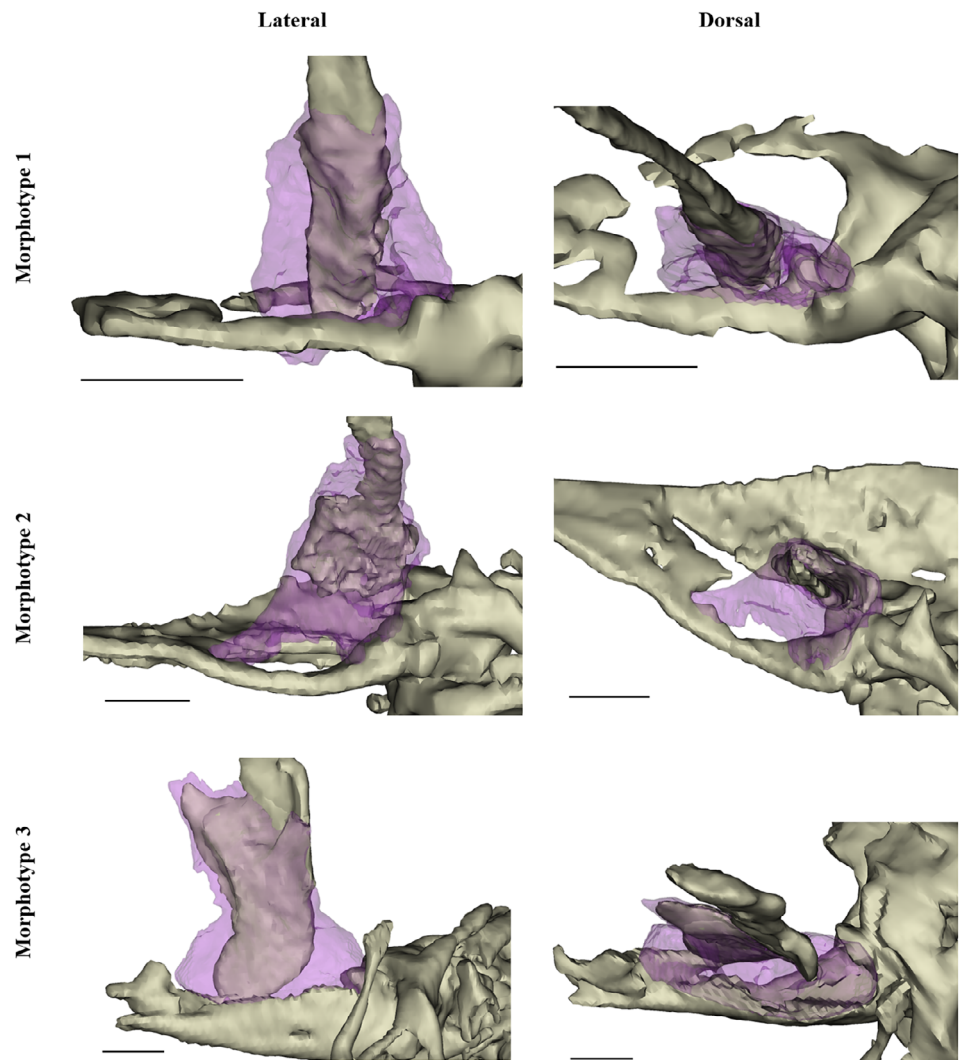
dome formed by the fusion of the bilateral halves was not as high and curved as in M1-fishes, and in the two *Hemimyzon*, was nearly flat. The posterior processes of the basipterygium in nearly all species (*Homalopteroides nebulosus* had posterior processes resembling those in M1) were only about half as long as those observed in M1-fishes and ended with a blunt taper caudally, as opposed to a long point.

3.1.4 | Balitorid Morphotype 3

Eleven species were categorized into a third morphotype (M3; Table 1; Figure 2, Row 4), which included species with the most extreme differences from the typical teleost pelvic morphology (*Balitora burmanica*, *Balitora* sp., *Balitoropsis ophiolepis*, *Bhavana australis*, *Cryptotora thamicola*, *Hemimyzon macropterus*, *Homalopteroides smithi*, *Homalopteroides stephensoni*, *Homalopteroides tweediei*, *Homalopteroides weberi*, and *Pseudohomaloptera leonardi*). Thoracic ribs

in M3-fishes had the largest vertebral contact area as compared to the other morphotypes and the cyprinid outgroup, and the angle of the contact area was closest to vertical, extending from the anteroventral parapophysis to the diapophysis located at the base of the neural spine. Zygapophyses were robust and had articulating facets significantly larger than those seen in M1 and M2, with anterior zygapophyses averaging 23.75% ($n = 11$, $SD = 0.04$) and posterior zygapophyses averaging 12.67% ($n = 11$, $SD = 0.05$) of the vertebral length. The first caudal vertebra, directly following the vertebrae supporting the sacral ribs, had anterior zygapophyses articulating with the sacral vertebrae and reduced posterior zygapophyses. The sacral rib was more robust than the thoracic ribs preceding it, thicker throughout its length, and extended in a large flared crest near its midpoint. The distal end of the sacral rib was firmly attached to basipterygium at the lateral foramina via ligamentous attachment (Figure 8). Similar to M2, the basipterygium was nearly as wide as it was long, with average width 96.54% of length ($n = 11$, $SD = 0.12$),

FIGURE 8 Lateral and dorsal views of the distal ligament connecting the sacral rib to the lateral foramina of the basiptyergium. Morphotype 1, *Homaloptera ogilviei* (USNM 288431); Morphotype 2, *Homalopterula ripleyi* (USNM 390014); and Morphotype 3, *Balitora* sp. (ANSP 179834); ligament (transparent purple); bone (tan), scale bars = 0.5 mm



and the central region of the plate, where the two halves joined at the midline, was the least domed of the balitorid fishes and the lateral edges of the basiptyergium anterior to the fin rays were curved dorsally. Posterior processes of the basiptyergium were on average smaller than those in the other two morphotypes, with some lacking these processes completely. While the intermuscular bones in other morphotypes, as compared to outgroup teleosts, were largely unremarkable, in M3 fishes they were thick and often attached to the lateral aspect of the vertebral centra. Morphotypes 1 and 2 did not show a consistent pattern in neural spine shape. However, in M3, the neural spines anterior to the dorsal fin were broadened, with the extent varying from only slightly, about 25% of the spine height in *Homalopteroides smithi*, to 100% of the spine height in *Balitora burmanica* and *Balitoropsis ophiolepis*.

3.2 | Shape variation and PCA

Shape variation using Elliptical Fourier Analysis of rib shape outlines accounts for 82.06% of the variance observed in morphotype variation of rib shape within the first three principal component axes

(Figure 3). Principal component 1 describes 47.56% of the shape variation in the thickness of the rib with the low values showing long and narrow ribs, and the higher values showing stockier, thickened ribs with the thickened crest distinctive of M3 (Figure 3, top row). Principal component 2 (Figure 3, second row) describes 22.45% of the shape variation with low values indicating ribs with less curvature and a more flattened shape and high values indicating ribs with highly arched shape and an increased area below the rib with increased curvature. Principal component 3 describes 12.05% of the variation in the shape of the rib near the attachment to the vertebrae and the mediolateral location of the crest relative to the rib attachment site to the vertebra (Figure 3, third row). Other PC axes illustrate variation in the location of the crest and size of the vertebrae attachment (Figure 3, PC 4–5 and Supporting information 1, Table S2).

The morphospace determined by the shape analysis using Elliptical Fourier Analyses indicates distinct spatial separations among the three morphotypes (Figure 4). Results of the LDA explain 89.81% and 10.19% of the among-group variation in LD1 and LD2 (Supporting information 1, Figure S1), respectively, with a resubstitution accuracy of 1.0 and a jackknifed (leave-one-out) accuracy of 0.857. The reduced accuracy of the jackknifed LDA will likely impact species

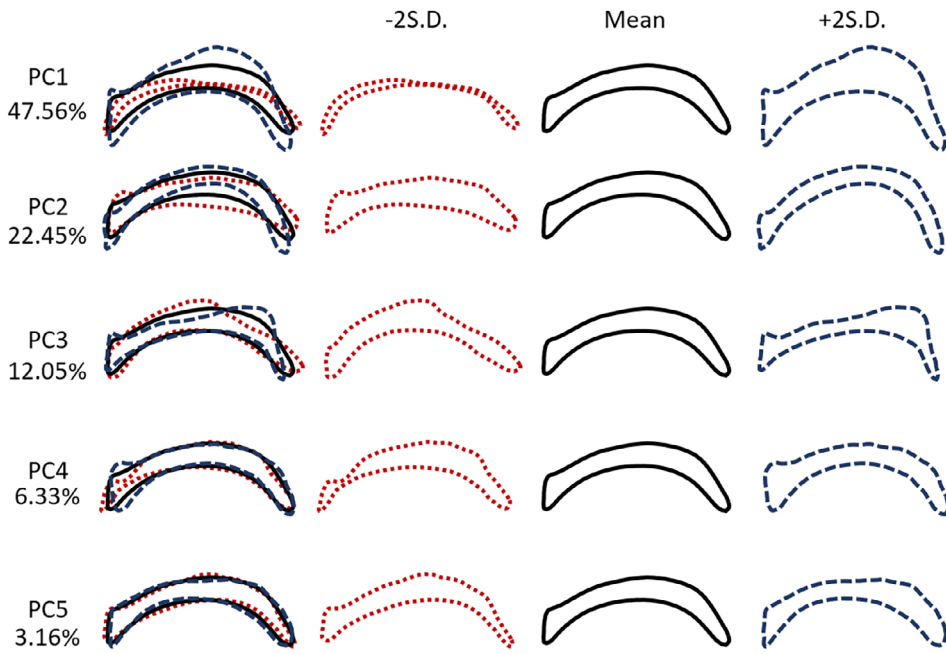


FIGURE 3 Visualization of the rib shape variation explained by PCs 1–5 at ± 2 SD and the mean shape for each with overlay at left and the percent of shape variance explained given for each PC

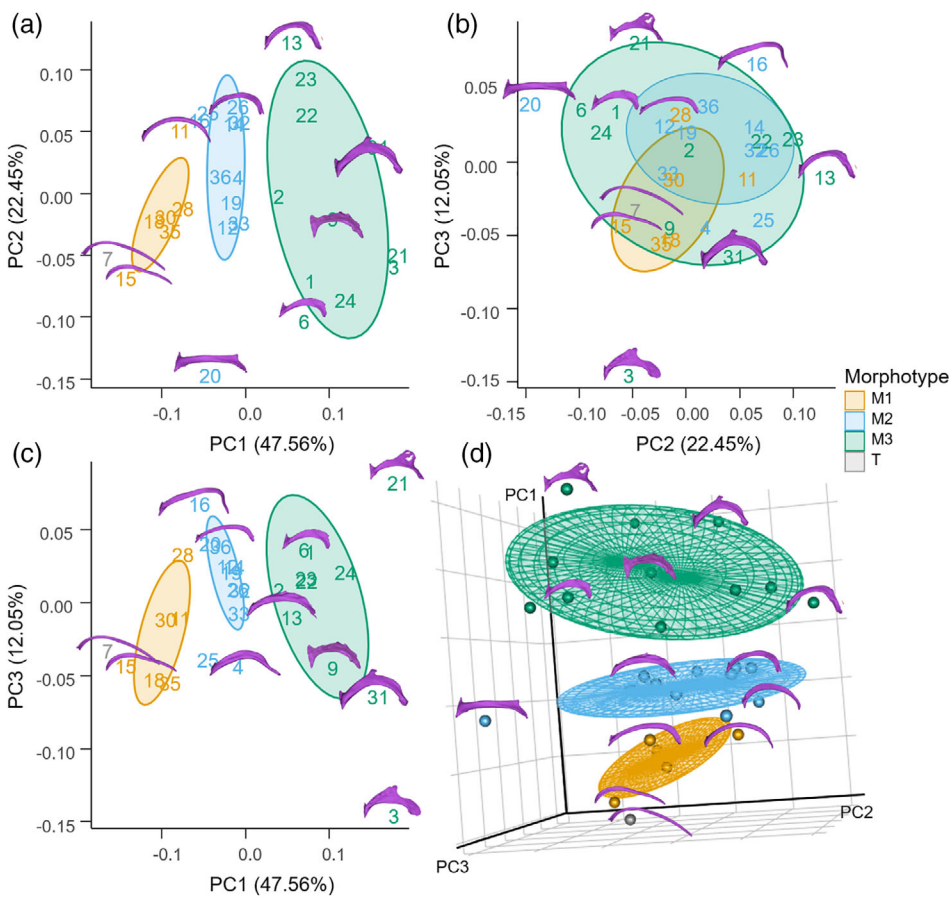


FIGURE 4 Results of the principal components analyses of rib shape using Elliptical Fourier Analyses for inferring morphotypes of balitorid loaches. (a) Morphospace represented by the bivariate graph of PC1 and PC2 scores; (b) morphospace represented by the bivariate graph of PC1 and PC3 scores; (c) morphospace represented by the bivariate graph of PC2 and PC3 scores; and (d) 3-Dimensional morphospace represented by the 3D plot of PC1, PC2, and PC3 with ellipses representing two standard deviations from the mean shape. See Supplemental Material 1 Table 4 for identification of numbered species in (a–c)

which are either on the extremes of the shape variation (outliers) or are on the edge of the boundaries of two morphotypes. Principal component 1 shows significant differences between the balitorid morphotypes ($p < .002$ for all morphotype comparisons except for M1

against typical teleost rib morphology) with greater overlap among morphotype space observed in PCs 2 and 3. Along PC1 (47.56%), M1 is grouped towards the end of the axis representing long and narrow sacral ribs and small vertebral attachment area, M2 in the center with

thicker ribs and intermediate attachment area, and M3 at the other end of the axis representing enlarged ribs and a flared crest (Figure 3, top row and Figure 4). For the PC2 axis (22.45%) M3-species were evenly distributed along the axis of the principal component, including species with ribs of both minimal curvature (*Bhavana australis*, Figure 4, #6) and tight curvature (*Hemimyzon macropterus*, Figure 4, #13). M2 has a more constrained range along PC2 with the greatest difference between *Homalopteroides rupicola* (Figure 4, #20) and *Homalopterula riplei* (Figure 4, #26). Along PC2, M1 is even more restricted to the central area of space with curvature closer to the mean shape (Figure 4) of all species analyzed. Most of the PC3 axis (12.05%) for M3 defines the location of the flared crest of the rib with the two extremes within M3 illustrated by *Balitoropsis ophiolepis* (Figure 4, #3) and *Homalopteroides smithi* (Figure 4, #21). M1-variation along PC3 shows the location of the major bend in the rib along the mediolateral axis.

3.3 | Muscle morphology

The axial body wall muscles (Figure 5, grey) exhibited the typical fish w-shaped myomere configuration and its two hypaxial subdivisions, the *musculus obliquus superioris* and *m. obliquus inferioris* (Winterbottom 1973), were readily distinguished in the μ CT-scans. The obliquus superioris muscle fibers were oriented anterodorsally to posteroventrally whereas the obliquus inferioris muscle fibers were oriented anteroventrally to posteriodorsally. In M2 and M3, the distal end of the sacral rib passes superficial to the obliquus before inserting into the basipterygium (Figure 5a); this lateral supraposition is not as pronounced as in M1. In our example of a typical teleost, this opening is not visible and the ribs do not pass through the body wall to reach the basipterygium; instead they are deep to the obliquus superioris (Figure 5a, grey). In contrast to the teleost outgroup, which had small infracarinalis muscles, fishes in all three balitorid morphotypes had thick infracarinalis anterior and infracarinalis medius muscles, which were connected by a thin ligament along the ventral side of the pelvis (Figure 5a, pink). The extensor proprius (Figure 5, green), which is part of the muscular sling holding the pelvis in place in typical teleosts, was not found in any of the balitorids stained with PTA.

We found large arrector muscles in all three morphotypes, although both the *m. arrector dorsalis* (Figure 5, fuchsia) and *m. arrector ventralis* (Figure 5, orange) have a greater physiological cross-sectional area in M2 and M3 than in M1 or in the typical teleost. The *m. arrector dorsalis* originates at the dorsolateral edge of the basipterygium following the anterolateral edge of the basipterygium and inserts on the first fin ray.

In M1, the *m. adductor superficialis* (Figure 5, purple) extended anteriorly on the lateral edge whereas M2 had some, although less of an extension anteriorly compared to the placement of the *m. adductor profundus* (Figure 5, yellow). Adductor profundus muscle origin placement on the basipterygium was near the midline of the basipterygium in M1 and M2; however, in M3, the origin was more lateral (Figure 5c). We found that the *m. adductor superficialis* and

m. adductor profundus tightly follow the curvature of the posterior edge of the basipterygium in all morphotypes. In M3, the dorsal pelvic muscles do not meet at the midline as seen in the other morphotypes and in other fishes. The *m. extensor proprius* (Figure 5, green), which is part of the muscular sling holding the pelvis in place in typical teleosts, was not found in any of the balitorids stained with PTA.

With the broadening of the basipterygium from M1 through M3, there is a shallower angle of the muscle fibers, with the adductor and abductor muscles of M1 being steepest, those of M2 having intermediate muscle fiber angles and those of M3 closest to horizontal. The *m. abductor profundus* in the balitorid fishes fills in the area underneath the concavity of the basipterygium leading to an increase in muscle volume in M2 and M3 which have a larger concavity volume (Figure 5b, turquoise).

3.4 | Physiological cross-sectional area

The physiological cross-sectional area (PCSA) of the pelvic muscles of balitorids is overall greater when compared to the outgroup teleost, *Carassius auratus* (Figure 6 and Supporting information, Table S3). Among the balitorid fishes, M1 had pelvic muscle PCSAs most similar to that of a typical fish, whereas M2 and M3 had greater PCSAs indicative of increased potential maximum force production within these muscles. Overall, PCSA of all pelvic muscles in M1 indicate a lower capacity for force production than all pelvic muscles in M2 and M3. Fiber length range varied between the morphotypes as well, with M2 exhibiting the greatest variability in fiber lengths and M3 fiber length falling in the median among the fishes analyzed. Morphotype 3 had the largest PCSA of all muscles except for the *m. adductor superficialis*, which was greatest in M2. The abductor and adductor muscles of M1 had low PCSA and short fiber lengths, indicating smaller maximum force production and limited range of movement while the arrector muscles had longer fiber lengths and thus a potential for greater range of motion. The large PCSA of the abductor profundus in M2 and M3, nearly three times that calculated for the same muscle in M1, indicates an increase in the potential maximum force exerted by the muscle and thus potentially an increased ability to position their fins under the body in support of their body for locomotion. Although the PCSA of all muscles are smaller in M1 than M2 or M3, the extent of the difference varies among the muscles (Figure 6b). Most muscles in M1 show a PCSA 34.15% that of the PCSA in M2 or M3, however, the superficial abductor muscle in M1 is similar in PCSA as found in M2 (89.82%) and in the superficial adductor, the PCSA of M1 is about 70.22% of that in M2 or M3.

3.5 | Phylogenomic relationships

The multispecies coalescent tree and the Maximum Likelihood phylogenetic reconstruction (Figure 7 and Supporting information 2, Figures S1 and S2) had identical topologies, and we matched the morphotypes to their position on the multispecies coalescent tree

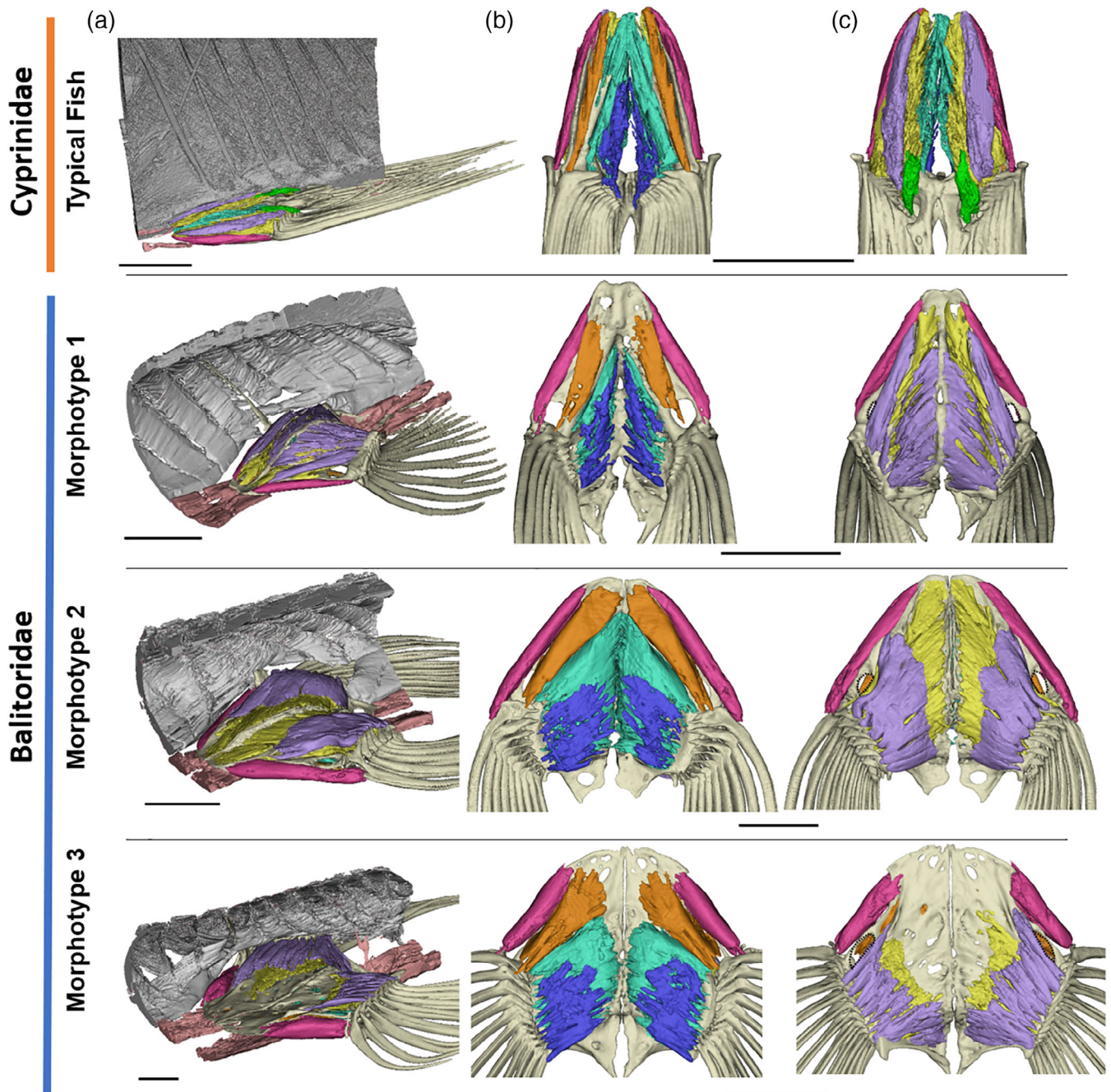


FIGURE 5 Pelvic girdle musculature from CT scans with PTA staining. Bony structures of the basipterygium and fin rays are inserted from CT scans of the same specimens prior to staining. Typical fish morphology, *Carassius auratus* (Flammang Lab); Morphotype 1, *Homaloptera ogilviei* (USNM 288431); Morphotype 2, *Homalopterula ripleyi* (USNM 390014); and Morphotype 3, *Balitora* sp. (ANSP 179834). (a) Lateral view shows the pelvis with the axial muscles and the sacral rib (red), (b) ventral and (c) dorsal views show segmented pelvic muscles (anterior to the top). Axial muscles (gray); infracarinalis (pink) abductor superficialis (blue); abductor profundus (turquoise); adductor profundus (yellow); adductor superficialis (purple); arrector dorsalis (fuchsia); arrector ventralis (orange); extensor proprius (green); and bone (tan), sacral rib insertion (black dotted outline). Scale bars. Scale bars = 2.5 mm

(Figure 7). Balitoridae is resolved as monophyletic and sister to a clade consisting of Gastromyzontidae and Serpenticobitidae. This clade is sister to the stone loach family Nemacheilidae. We recovered many of the same relationships (Figure 7 and Supporting information 2, Figure S1) within Balitoridae as the molecular phylogeny presented in Randall and Page (2015). We have expanded the phylogeny from

Randall and Page (2015) by including *Cryptotora* and *Neohomaloptera*. Within Balitoridae two subfamilies have strong support: Homalopteroidinae Randall and Page 2015 (*Homalopteroides*, *Homalopterula*, and *Neohomaloptera*) and Balitorinae Swainson 1839 (*Balitora*, *Hemimyzon*, *Sinogastromyzon*, *Cryptotora*, *Homaloptera*, *Balitoropsis*, and *Pseudohomaloptera*). Within Balitorinae, two major

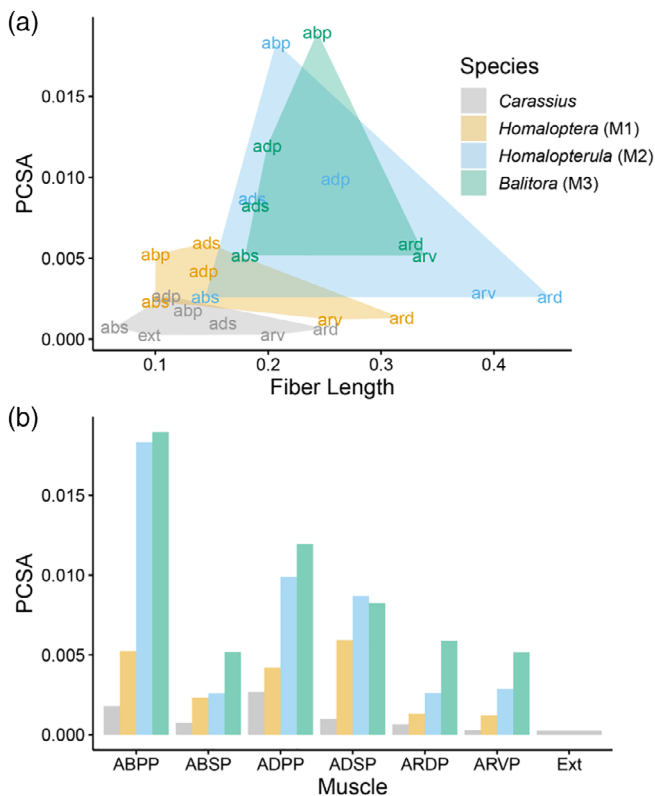


FIGURE 6 Biplot (a) of functional morphospace of normalized pelvic muscle physiological cross sectional area and fiber length for representative balitorids and *Carassius auratus* and barplot (b) of PCSA by muscle. Physiological cross sectional area values are normalized to total body volume using $V2/3$. Muscle abbreviations are as follows: abductor profundus (ABP), abductor superficialis (ABS), adductor profundus (ADP), adductor superficialis (ADS), arrector dorsalis (ARD), arrector ventralis (ARV), and extensor proprius (Ext)

clades are resolved: a strongly supported clade consisting of *Cryptotora* as the sister group to *Sinogastromyzon*, *Hemimyzon*, and *Balitora*, and a weakly supported clade consisting of *Pseudohomaloptera* as the sister group to *Balitoropsis* plus *Homaloptera*.

Although there are some sampling differences between our morphological and molecular datasets, all three morphotypes are included within the two subfamilies. The morphotypes (as grouped by the LDA) (Figure 7). The clade containing *Cryptotora*, *Balitora*, *Hemimyzon*, and *Sinogastromyzon* includes M2 and M3, while the clade containing *Homaloptera*, *Balitoropsis*, and *Pseudohomaloptera* contains all three morphotypes. The clade containing *Homalopteroides* includes M2 and M3, while the clade containing *Neohomaloptera* and *Homalopterula* includes M1 and M2. Two pairs of sister species share different morphotypes: *Balitoropsis zollingeri* and *B. ophiolepis* (M2 and M3, respectively) and *Homalopteroides tweediei* and *H. nebulosus* (M3 and M2, respectively). One of four species of *Homalopterula* (*Homalopterula vanderbilti*, not sampled in Figure 7) grouped into M1 while the other three were M2 and two of five species of *Homalopteroides* grouped in M2 while the other four were in M3. We did not find significant phylogenetic signal in the distribution of morphotypes both with and without the M1 specimens (with M1, $p = .365$, without M1, $p = .314$).

We found 7.00 observed evolutionary transitions with a randomization median of 8.00.

4 | DISCUSSION

Terrestrial excursions by fishes are observed throughout the teleost tree of life and include varying forms of locomotion (Wright & Turko, 2016). Methods used to move across terrestrial environments range from simply modified swimming, undulating or flipping the body as seen in eels (Gillis, 1998), sticklebacks (Clardy, 2012), and killifishes (Gibb, Ashley-Ross, & Hsieh, 2013; Gibb, Ashley-Ross, Pace, & Long, 2011); moving on land by crutching as in mudskippers (Kawano & Blob, 2013; Pace & Gibb, 2009) or pectoral fin-driven forward propulsion with undulation of the posterior body as in *Polypterus* (Standen, Du, & Larsson, 2014); to using alternating pelvic fin movements to generate forward momentum, as seen in lungfishes (King, Shubin, Coates, & Hale, 2011). The balitorid *Cryptotora thamicola* walks with a lateral-sequence-diagonal-couplets (LSDC) gait similar to that observed in salamanders, which is a unique form of terrestrial locomotion among fishes (Flammang et al., 2016). This locomotion is likely due to the fact that *Cryptotora thamicola* shares several morphological features with terrestrial tetrapods, including a robust pelvic girdle rigidly attached to the axial skeleton via a sacral rib, broad neural spines, and zygapophyses connecting serial vertebrae (Flammang et al., 2016).

4.1 | Balitorid pelvic skeleton

Unlike typical teleost fishes in which the bones of the pelvic fins are either suspended in a muscular sling or anteriorly attached to the pectoral girdle (Stiassny & Moore, 1992; Yamanoue et al., 2010), the bones of the pelvic fins in the balitorid species studied here (representing 14 of 16 genera) are connected to the axial skeleton via an elongated and/or enlarged sacral rib. Enlargement of the rib associated with the basipterygium is seen in Balitoridae and has also been reported in its sister family Gastromyzontidae (Conway, 2011; Sawada, 1982 [recognized as the balitorid subfamily, Gastromyzontinae]). In a morphological phylogenetic analysis, Conway (2011) reported an enlarged rib associated with the basipterygium as a character (117) that supports the monophyly of Balitoridae (recognizing Gastromyzontidae as a subfamily of Balitoridae). This character was also recognized as being independently gained in the family Psilorhynchidae, and the taxon *Garra dembeensis* (Conway, 2011), both found in fast-flowing riverine habitats similar to hill-stream loaches.

Mapping the morphotypes to the UCE phylogeny (Figure 7) shows that sacral rib shape varies along balitorid phylogenetic relationships with all three morphotypes showing up in both subfamilies Balitorinae and Homalopteroidinae. The two species from M1 (*Homaloptera ogilviei* and *Neohomaloptera johorensis*) are found in two different subfamilies whereas M2 and M3 are dispersed throughout

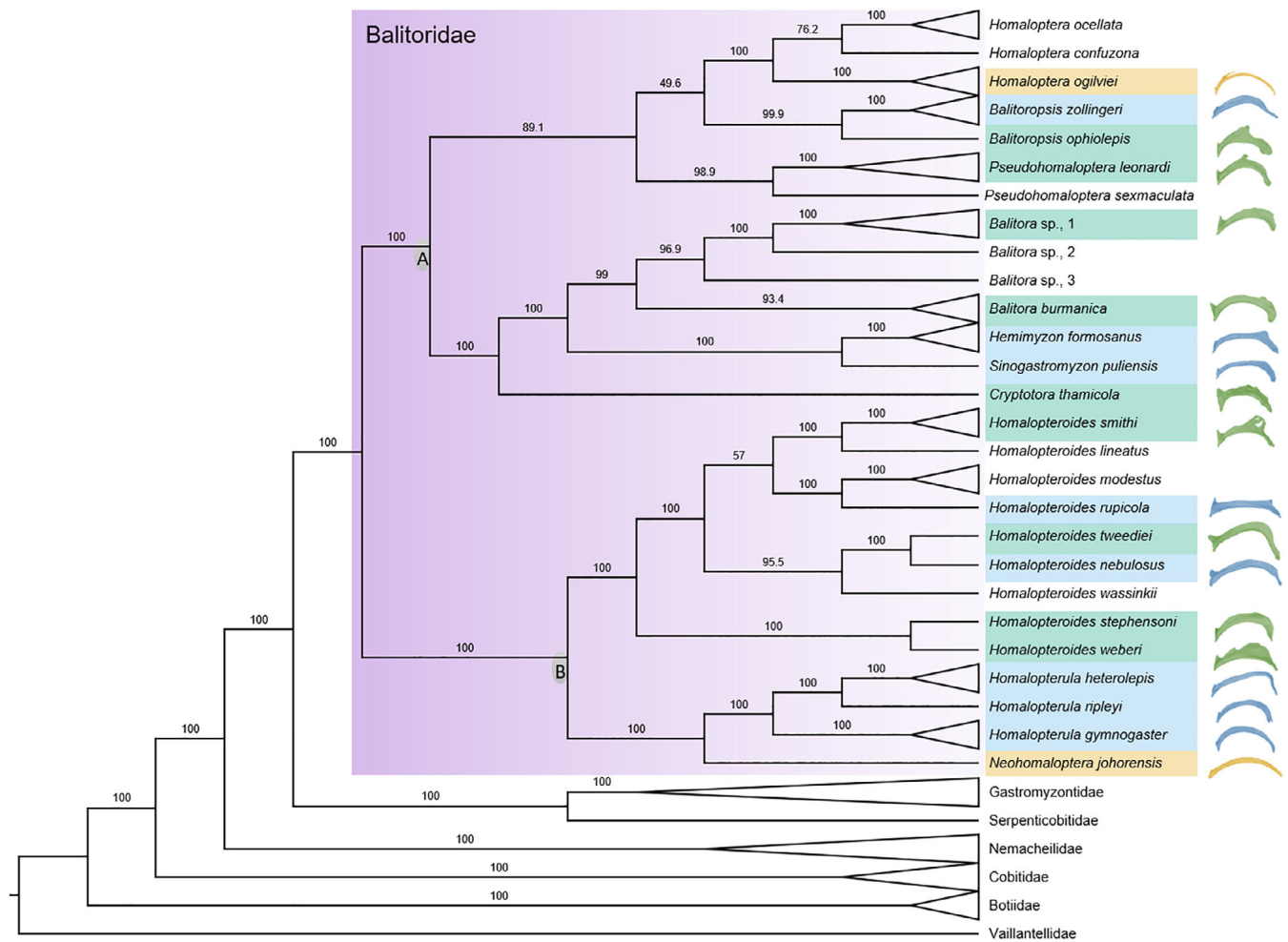


FIGURE 7 SVDQuartets tree of Balitoridae with boxes highlighting known rib morphotypes, Morphotype 1, yellow; Morphotype 2, blue; and Morphotype 3, green. Species without color coding have not been analyzed for morphotype. (a) Balitorinae and (b) Homalopteroidinae

Balitoridae. Based on the current sampling in this study, with the exception of *Homaloptera*, the groupings of described morphotypes M1–M3 do not reflect current phylogenetic relationships at the generic level (when more than two species were sampled within a genus; Figure 7). Three of the genera studied (*Homalopterula*, *Homalopteroides*, and *Balitoropsis*; Table 1 and Figure 7) have species separating into different morphotypes. It is worth noting that no genus encompassed both M1 and M3, however, suggesting that while the morphological differences may reflect a spectrum, variation was consistently directional, as observed through the PCA-results (Figure 4). More morphological and molecular samples of Balitoridae, Gastromyzontidae, Serpenticobitidae, and Barbuccidae are needed in order to perform a robust character ancestral state reconstruction and assess if an enlargement of the rib associated with the basipterygium is a character that unites Balitoridae (sensu lato of Tan & Armbruster, 2018).

The rib shape variation among the three morphotypes (Figures 2–4) is largely explained (PC1, 47.56%) by the differences in thickness of the sacral rib and the presence or absence of an enlarged crest. Thicker ribs connecting the pelvis to the vertebrae allow for a

greater transmission of forces from the pelvis to the axial skeleton, and support of the weight of the fish when out of the water (as reported for *Cryptotora* in Flammang et al., 2016) or counteracting a strong current. Increased robustness of the pelvis and its connection to the vertebral column was important in the evolution of terrestrial walking in tetrapods (King et al., 2011; Lebedev, 1997) as was the development of stronger pelvic musculature (Cole et al., 2011). These thicker ribs have a larger cross-sectional area, leading to increased strength in the bone (Hyman & Wake, 1992) and an increased force resistance (Blob & Biewener, 1999). The flared crest seen in M3 offers an increased surface area for muscle attachment at the pelvis. This flared crest is most often observed on the lateral portion of the rib at the point where the rib turns down toward the basipterygium although one species, *Balitoropsis ophiolepis* (Figure 4, #3), has a more medial crest. Increased contact area via enlarged fin rays and the dorsoventrally flattened body increases the frictional surface and promotes adhesion (Chang, 1945; Hora, 1930; Sawada, 1982). From the linear discriminant analysis, the morphotype of species not yet analyzed here could be predicted with high accuracy (0.857 from the jackknifed analysis, 1.0 from the resubstitution analysis) as

accessibility to specimens and scanning facilities increases. Species which fall near the bounds of the morphotypes or have more extreme shape variations will be more difficult to place into the discrete morphotypes.

The pre- and post-zygapophyses seen in varying degrees in M1 and present in M2 and M3 have been recorded in highly rheophilic species (He, Gayet, & Meunier, 1999; Lujan & Conway, 2015; Sawada, 1982). Reinforcement of the vertebral column via processes between serial vertebrae is seen in different groups of rheophilic fishes and theorized to be specialized for this habitat (Lujan & Conway, 2015). In addition to the zygapophyses strengthening the axial skeleton, broadening of the neural spines was seen in one species of M1 (*Homaloptera orthogoniata*) three species of M2 (*Balitoropsis zollingeri*, *Hemimyzon formosanus*, and *Hemimyzon taitungensis*) and in all M3 species. This broadening of the neural spines, like the enlargement of a flared crest in the sacral rib, increases surface area for muscle attachment; in tetrapods broad neural spines support a system of ligaments that reinforce the stiffness of the axial skeleton and help counteract the effect of gravity on the abdomen.

4.2 | Balitorid pelvic musculature

In the pelvic muscles of the fishes studied here, as the basipterygium becomes broader compared to its length, we see more shallow fiber angles in the adductor and abductor muscles. This change in fiber angle and the increased size of the muscles increase the maximum force of the contraction of these muscles that may help the pelvic fins adhere to the substrate and keep the fish from being carried downstream (Chang, 1945). The absence of the *m. extensor proprius* in balitorids is unsurprising as it is often absent in benthic fishes (Stiassny & Moore, 1992; Winterbottom, 1973; Yamanoue et al., 2010).

In M3, the dorsal pelvic muscles do not appear to meet at the midline as seen in M1, M2, and typical fishes (represented here as *C. auratus*). This could be from inconsistent staining in the individuals examined and increased coverage of individuals is necessary to determine if this is real or an artifact. Nonetheless, the normalized muscle volume and PCSAs are still greater for nearly all of the muscles in M3.

Higher PCSA values indicate a greater capacity for force in fishes with enlarged sacral ribs (M2 and M3). In M3, all muscles, except for the *m. adductor superficialis*, had the greatest PCSA values, whereas *Carassius auratus*, representing typical fish morphology, had the lowest PCSA for all muscles. Moving from a typical teleost to M1, M2, then M3, PCSA increased as expected with increased area of the basipterygium and thus, more space for muscle attachment. The *m. abductor profundus* (Figure 5b, turquoise) has the largest PCSA in M2 and M3, largely due to increased volume of muscle originating from the basipterygium concavity. The increased force capacity in M2 and M3 may indicate an increased ability to hold place in fast-flowing water and is presumed to indicate an increased ability to perform walking behaviors. The morphospace of the potential muscle force (PCSA) and range of extension in the muscles (fiber length; Figure 6)

illustrate the tradeoffs between these two metrics of muscle architecture and function. The long fiber lengths and relatively low PCSA values for the arrector muscles in all four species studied allows for larger movements of the first fin ray but lower power producing the movement. The deep adductor and abductor muscles of M2 and M3 have the largest PCSA values of all muscles measured and all have moderate fiber lengths, these muscles generate the most power of the pelvic muscles with the highest PCSA in the deep abductors, which may be important for gripping to the substrate with the fin rays and would facilitate positioning the fins under the body in support of walking.

The sacral rib is held securely in place by a ligament encapsulating the distal end of the rib and connecting it to the basipterygium within the lateral foramen. In addition to increasing the radiopacity of the musculature, PTA staining highlighted the connective ligament holding the enlarged sacral rib in place in all three morphotypes (Figure 8). This ligament was also found during dissection of specimens from M1 (*Homaloptera parclitella*) and M3 (*Homalopteroides tweediei*). In the dissections, the ligament firmly held the rib in place at the lateral edge of the lateral foramen of the basipterygium. The ligament was larger in M3 than in M1, encapsulating a larger proportion of the distal end of the rib. In addition, the distal end of the sacral rib in M3 is larger and rounded, as opposed to coming to a tapered point as in the M1 fish. The increased size of the ligament reduces the amount of movement possible at the distal end of the rib and likely increases the stability of the rib-basipterygium connection. The ligament connecting the sacral rib and the basipterygium has been noted before and was presumed to support the enlarged basipterygium, helping to maintain the large ventral surface of the pelvic region (Chang, 1945; Sawada, 1982).

4.3 | Ecology and phylogeny of balitorid morphotypes

The present study examined the skeletal morphology of a broad sampling of balitorid fishes, which resulted in the delimitation of three morphotypes. The structures that support the different morphotypes are expected to have major implications for the biomechanics of the terrestrial locomotion behaviors observed in this family. Testing for phylogenetic signal indicates that the morphotype groupings are not congruent with evolutionary relationships. From the lack of phylogenetic signal, we can conclude that the variation in pelvic structures in balitorid loaches are independent adaptations in response to a rheophilic environment (Lujan & Conway, 2015).

In addition to the selection for enlarged sacral ribs and connectivity between the pelvis and the axial skeleton, the wide range of pelvic morphology seen within the family may indicate adaptive phenotypic plasticity; however, determining this requires more study. Phenotypic plasticity, or changes in an organism as a result of interactions with its environment, can lead to the evolution of adaptations and specializations (Pigliucci, Murren, & Schlichting, 2006; West-Eberhard, 1989). Phenotypic plasticity in teleost skeletal and muscular structures has been observed in response to changes in loading systems on fin

structures, muscular structures, feeding morphology, and the development of intermuscular bones (Danos & Ward, 2012; Hegrenes, 2001; McFarlane, Rossi, & Wright, 2019; Standen et al., 2014). Unfortunately, while the fishes here are all classified as hill-stream loaches, at this time there are no published details regarding their habitats through ontogeny or over time that would allow for further investigation into the environmental forces with which these fishes interact.

Although balitorids are well documented in museum collections and some species are commonly collected for the pet trade, little is known about the details of their various habitats, particularly how physical parameters of the habitat change between the wet and dry season. These loaches are known to be from fast-flowing rivers and streams in 11 countries (Cambodia, China, India, Indonesia (Borneo, Java, and Sumatra), Laos, Malaysia (peninsular and Borneo), Myanmar, Nepal, Taiwan, Thailand, and Vietnam) and are often found on rocky substrates, but the flow rates and physical properties of their habitats are not well known (Alfred, 1969; Dudgeon, 2000; Kottelat, 2012; Trajano et al., 2002). Alfred (1969) remarked on the substrate and water velocity preference for some species on the Malay peninsula, and his findings of velocity preference align with our morphotype findings with M1 (*Homaloptera ogilviei* and *Homaloptera orthogoniata*) preferring lower velocities, and M2 and M3 (*Balitoropsis zollingeri* and *Pseudohomaloptera leonardi*, respectively) preferring higher velocities. More recently, a study on the physical parameters of balitorid and nemacheilid loaches in central Thailand found that water velocity was not significantly different in habitats occupied by the species studied (Beamish, Sa-ardrit, & Cheevaporn, 2008); however, that study included many nemacheilids which do not possess the enlarged sacral rib and may have impacted the findings. A more inclusive review of water flow rates and substrate structure of balitorid habitats will greatly aid in our understanding of the ecology of these fishes.

A strong hypothesis for evolutionary relationships is critical for accurate comparative study (Garland, Bennett, & Rezende, 2005; Sanford, Lutterschmidt, & Hutchison, 2002), and we have reconstructed our own evolutionary hypothesis of balitorids using phylogenomic data. This is the first investigation to include the cave-inhabiting *Cryptotora thamicola* and recover it as belonging to the subfamily Balitorinae. Further study into the phylogenetic relationships and the biomechanics of the unique walking behavior observed in these fishes will provide an opportunity to increase our knowledge of morphological evolution in balitorids.

ACKNOWLEDGMENTS

We would like to thank J. Gladman at Duke University, M. Hill at the AMNH, and B. Ache at Microphotonics for their assistance with collecting μ CT scans and to the oVert TCN (DBI 1701714) for providing some of the scans used in this study. Thank you to J. Williams and S. Smith at the Smithsonian, M. Stiassny at the AMNH, M. Sabaj and M. Arce at the ANSP, and D. Catania at the California Academy of Sciences for assistance in obtaining specimen loans for this project. The SLBB-f Hackathon working group at Rutgers-Newark/NJIT was instrumental to completing the analyses for this study. This study was heavily influenced by J. Markiewicz's work on the reconstruction of

an early *Cryptotora thamicola* μ CT scan and by D. Soares' recommendation to BEF to investigate the walking behavior of *Cryptotora*. Funding for this research included the National Science Foundation Understanding the Rules of Life Grant #1839915 (awarded to BEF, PC, and LMP), Duke University RTNN Free Use Award, ASIH Raney Award, AMNH Lerner-Gray Grant, and Sigma Xi GIAR (awarded to CHC). We greatly appreciate the permissions granted by federal and other governmental agencies in Thailand to A. Suvarnaksha and S. Tongnunui at the Kanchanaburi Campus of Mahidol University, to conduct fieldwork and collect fishes necessary for this study.

CONFLICT OF INTEREST

The authors have no conflict of interest to declare.







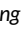
AUTHOR CONTRIBUTIONS

Callie Crawford: Conceptualization; data curation; formal analysis; funding acquisition; investigation; methodology; project administration; visualization; writing-original draft; writing-review and editing. **Zachary Randall:** Data curation; investigation; methodology; validation; visualization; writing-review and editing. **Pamela Hart:** Data curation; formal analysis; methodology; visualization; writing-review and editing. **Lawrence Page:** Data curation; funding acquisition; investigation; resources; writing-review and editing. **Prosanta Chakrabarty:** Data curation; formal analysis; funding acquisition; resources; software; supervision; writing-review and editing. **Apinun Suvarnaksha:** Investigation; resources; writing-review and editing. **Brooke Flammang:** Conceptualization; funding acquisition; investigation; methodology; project administration; resources; software; supervision; writing-original draft; writing-review and editing.

DATA AVAILABILITY STATEMENT

Data Availability Statement Data Accessibility Statement The CT scan data that support the findings of this study are openly available in MorphoSource.org at www.morphosource.org, reference numbers M13737, M14876, M15050, M15107, M15110, M15116, M15120, M15126, M15127, M15164, M15493, M19663, M22168, M53469, M53472, M53476, M53479, M53481, M53484, M53485, M53485, M53489, M53490, M53491, M53492, M53493, M53494, M53495, M53497, and M53498. Raw sequence data for ultraconserved elements will be accessible on the Sequence Read Archive from the National Center for Biotechnology Information. Molecular specimen accession and catalog numbers are available in the Supplementary Material.

ORCID

Callie H. Crawford  <https://orcid.org/0000-0002-7225-8137>
 Zachary S. Randall  <https://orcid.org/0000-0001-8973-3304>
 Pamela B. Hart  <https://orcid.org/0000-0002-4056-6864>
 Lawrence M. Page  <https://orcid.org/0000-0002-0658-5519>
 Prosanta Chakrabarty  <https://orcid.org/0000-0003-0565-0312>
 Apinun Suvarnaksha  <https://orcid.org/0000-0002-9186-9523>
 Brooke E. Flammang  <https://orcid.org/0000-0003-0049-965X>

REFERENCES

- Ahlberg, P. E. (2019). Follow the footprints and mind the gaps: A new look at the origin of tetrapods. *Earth and Environmental Science Transactions of the Royal Society of Edinburgh*, 109(1–2), 115–137. <https://doi.org/10.1017/s1755691018000695>
- Alfred, E. R. (1969). The Malayan cyprinoid fishes of the family Homalopteridae. *Zoologische Mededelingen*, 43(18), 213–237.
- Allen, V., Eelsey, R. M., Jones, N., Wright, J., & Hutchinson, J. R. (2010). Functional specialization and ontogenetic scaling of limb anatomy in *Alligator mississippiensis*. *Journal of Anatomy*, 216(4), 423–445. <https://doi.org/10.1111/j.1469-7580.2009.01202.x>
- Beamish, F. W. H., Sa-ardrit, P., & Cheevaporn, V. (2008). Habitat and abundance of Balitoridae in small rivers of Central Thailand. *Journal of Fish Biology*, 72(10), 2467–2484. <https://doi.org/10.1111/j.1095-8649.2008.01854.x>
- Blob, R. W., & Biewener, A. A. (1999). In vivo locomotor strain in the hindlimb bones of *Alligator mississippiensis* and *Iguana iguana*: Implications for the evolution of limb bone safety factor and non-sprawling limb posture. *Journal of Experimental Biology*, 202(9), 1023–1046.
- Blomberg, S. P., Garland, T., & Ives, A. R. (2003). Testing for phylogenetic signal in comparative data: Behavioral traits are more labile. *Evolution*, 57(4), 717–745. <https://doi.org/10.1111/j.0014-3820.2003.tb00285.x>
- Bush, S. E., Weckstein, J. D., Gustafsson, D. R., Allen, J., DiBlasi, E., Shreve, S. M., ... Johnson, K. P. (2016). Unlocking the black box of feather louse diversity: A molecular phylogeny of the hyper-diverse genus *Brueelia*. *Molecular Phylogenetics and Evolution*, 94, 737–751. <https://doi.org/10.1016/j.ympev.2015.09.015>
- Buytaert, J., Goyens, J., De Greef, D., Aerts, P., & Dirckx, J. (2014). Volume shrinkage of bone, brain and muscle tissue in sample preparation for micro-CT and light sheet fluorescence microscopy (LSFM). *Microscopy and Microanalysis*, 20(4), 1208–1217. <https://doi.org/10.1017/S1431927614001329>
- Chang, H. (1945). Comparative study on the girdles and their adjacent structures in Chinese homalopterid fishes with special reference to the adaptation to torrential stream. *Sinensia*, 16, 9–26.
- Chifman, J., & Kubatko, L. (2014). Quartet inference from SNP data under the coalescent model. *Bioinformatics*, 30(23), 3317–3324. <https://doi.org/10.1093/bioinformatics/btu530>
- Clardy, T. R. (2012). Aquatic and terrestrial locomotion of the rock pricklyback, *Xiphister mucosus* (Cottiformes: Zoarcoidei: Stichaeidae). *Northwestern Naturalist*, 93(3), 203–210. <https://doi.org/10.1898/11-19.1>
- Cole, N. J., Hall, T. E., Don, E. K., Berger, S., Boisvert, C. A., Neyt, C., Ericsson R., Joss J., Gurevich D. B. Currie, P. D. (2011). Development and evolution of the muscles of the pelvic fin. *PLoS Biology*, 9(10), 1001168. <https://doi.org/10.1371/journal.pbio.1001168>, e1001168
- Conway, K. W. (2011). Osteology of the south Asian genus *Psilorhynchus* McClelland, 1839 (Teleostei: Ostariophysii: Psilorhynchidae), with investigation of its phylogenetic relationships within the order Cypriniformes. *Zoological Journal of the Linnean Society*, 163(1), 50–154. <https://doi.org/10.1111/j.1096-3642.2011.00698.x>
- Conway, K. W., Lujan, N. K., Lundberg, J. G., Mayden, R. L., & Siegel, D. S. (2012). Microanatomy of the paired-fin pads of ostariophysan fishes (Teleostei: Ostariophysii). *Journal of Morphology*, 273(10), 1127–1149. <https://doi.org/10.1002/jmor.20049>
- Danos, N., & Ward, A. B. (2012). The homology and origins of intermuscular bones in fishes: Phylogenetic or biomechanical determinants? *Biological Journal of the Linnean Society*, 106(3), 607–622. <https://doi.org/10.1111/j.1095-8312.2012.01893.x>
- de Meyer, J., & Geerinckx, T. (2014). Using the whole body as a sucker: Combining respiration and feeding with an attached lifestyle in hill stream loaches (Balitoridae, Cypriniformes). *Journal of Morphology*, 275(9), 1066–1079. <https://doi.org/10.1002/jmor.20286>
- Descamps, E., Sochacka, A., de Kegel, B., van Loo, D., Hoorebeke, L., & Adriaens, D. (2014). Soft tissue discrimination with contrast agents using micro-ct scanning. *Belgian Journal of Zoology*, 144(1), 20–40.
- Dickson, B. V., & Pierce, S. E. (2019). How (and why) fins turn into limbs: Insights from anglerfish. *Earth and Environmental Science Transactions of the Royal Society of Edinburgh*, 109(1–2), 87–103. <https://doi.org/10.1017/S1755691018000415>
- Dudgeon, D. (2000). The ecology of tropical Asian rivers and streams in relation to biodiversity conservation. *Annual Review of Ecology and Systematics*, 31, 239–263. <https://doi.org/10.1146/annurev.ecolsys.31.1.239>
- Faircloth, B. C., McCormack, J. E., Crawford, N. G., Harvey, M. G., Brumfield, R. T., & Glenn, T. C. (2012). Ultraconserved elements anchor thousands of genetic markers spanning multiple evolutionary timescales. *Systematic Biology*, 61(5), 717–726. <https://doi.org/10.1093/sysbio/sys004>
- Flammang, B. E., Suvannaraksha, A., Markiewicz, J., & Soares, D. (2016). Tetrapod-like pelvic girdle in a walking cavefish. *Scientific Reports*, 6, 23711. <https://doi.org/10.1038/srep23711>
- Fricke, R., Eschmeyer, W. N., & van der Laan, R. (2019). *Eschmeyer's catalog of fishes: genera, species, references*, San Francisco, USA: California Academy of Sciences. Retrieved from <http://researcharchive.calacademy.org/research/ichthyology/catalog/fishcatmain.asp>
- Garland, T., Bennett, A. F., & Rezende, E. L. (2005). Phylogenetic approaches in comparative physiology. *Journal of Experimental Biology*, 208, 3015–3035. <https://doi.org/10.1242/jeb.01745>
- Gibb, A. C., Ashley-Ross, M. A., & Hsieh, S. T. (2013). Thrash, flip, or jump: The behavioral and functional continuum of terrestrial locomotion in teleost fishes. *Integrative and Comparative Biology*, 53(2), 295–306. <https://doi.org/10.1093/icb/ict052>
- Gibb, A. C., Ashley-Ross, M. A., Pace, C. M., & Long, J. H. (2011). Fish out of water: Terrestrial jumping by fully aquatic fishes. *Journal of Experimental Zoology Part A: Ecological Genetics and Physiology*, 315A(10), 649–653. <https://doi.org/10.1002/jez.711>
- Gillis, G. B. (1998). Environmental effects on undulatory locomotion in the American eel *Anguilla rostrata*: Kinematics in water and on land. *Journal of Experimental Biology*, 201(7), 949–961.
- Hart, P. B., Niemiller, M. L., Burress, E. D., Armbruster, J. W., Ludt, W. B., Chakrabarty, P. (2020). Cave-adapted evolution in the north American amblyopsid fishes inferred using phylogenomics and geometric morphometrics. *Evolution*, 74(5), 936–949. <https://doi.org/10.1111/evo.13958>
- He, S., Gayet, M., & Meunier, F. J. (1999). Phylogeny of the Amphiliidae (Teleostei: Siluriformes). *Annales Des Sciences Naturelles: Zoologie et Biologie Animale*, 20(4), 117–146. [https://doi.org/10.1016/s0003-4339\(00\)88881-4](https://doi.org/10.1016/s0003-4339(00)88881-4)
- Hegrenes, S. (2001). Diet-induced phenotypic plasticity of feeding morphology in the orangespotted sunfish, *Lepomis humilis*. *Ecology of Freshwater Fish*, 10(1), 35–42. <https://doi.org/10.1034/j.1600-0633.2001.100105.x>
- Hora, S. L. (1930). Ecology, bionomics and evolution of the torrential fauna, with special reference to the organs of attachment. *Philosophical Transactions of the Royal Society B: Biological Sciences*, 218(450–461), 171–282. <https://doi.org/10.1098/rstb.1930.0005>
- Hora, S. L. (1932). Classification, bionomics and evolution of homalopterid fishes. *Memoirs of the Indian Museum*, 12, 263–330.
- Hyman, L., & Wake, M. (1992). *Hyman's comparative vertebrate anatomy*, Chicago, USA: University of Chicago Press.
- Iwata, H., & Ukai, Y. (2002). SHAPE: A computer program package for quantitative evaluation of biological shapes based on elliptic Fourier descriptors. *The Journal of Heredity*, 93(5), 384–385. <https://doi.org/10.1093/jhered/93.5.384>
- Kawano, S. M., & Blob, R. W. (2013). Propulsive forces of mudskipper fins and salamander limbs during terrestrial locomotion: Implications for

- the invasion of land. *Integrative and Comparative Biology*, 53(2), 283–294. <https://doi.org/10.1093/icb/ict051>
- King, H. M., Shubin, N. H., Coates, M. I., & Hale, M. E. (2011). Behavioral evidence for the evolution of walking and bounding before terrestriality in sarcopterygian fishes. *Proceedings of the National Academy of Sciences of the United States of America*, 108(52), 21146–21151. <https://doi.org/10.1073/pnas.1118669109>
- Kottelat, M. (2012). Conspectus cobitidum: An inventory of the loaches of the world (Teleostei: Cypriniformes: Cobitoidei). *Raffles Bulletin of Zoology*, 3, 1–82.
- Kuhl, F. P., & Giardina, C. R. (1982). Elliptic Fourier features of a closed contour. *Computer Graphics and Image Processing*, 18(3), 236–258. [https://doi.org/10.1016/0146-664X\(82\)90034-X](https://doi.org/10.1016/0146-664X(82)90034-X)
- Lanfear, R., Frandsen, P. B., Wright, A. M., Senfeld, T., & Calcott, B. (2017). Partitionfinder 2: New methods for selecting partitioned models of evolution for molecular and morphological phylogenetic analyses. *Molecular Biology and Evolution*, 34(3), 772–773. <https://doi.org/10.1093/molbev/msw260>
- Lebedev, O. A. (1997). Fins made for walking. *Nature*, 390, 21–22. <https://doi.org/10.1038/36215>
- Lieber, R. L. (2002). *Skeletal muscle structure, function, and plasticity*. Philadelphia, PA: Lippincott Williams & Wilkins.
- Lujan, N. K., & Conway, K. W. (2015). Life in the fast lane: A review of rheophily in freshwater fishes. In *Extremophile fishes: Ecology, evolution, and physiology of Teleosts in extreme environments* (pp. 107–136). Cham, Switzerland: Springer. https://doi.org/10.1007/978-3-319-13362-1_6
- Maddison, W. P., & Slatkin, M. (1991). Null models for the number of evolutionary steps in a character on a phylogenetic tree. *Evolution*, 45(5), 1184–1197. <https://doi.org/10.1111/j.1558-5646.1991.tb04385.x>
- McFarlane, W., Rossi, G. S., & Wright, P. A. (2019). Amphibious fish 'get a jump' on terrestrial locomotor performance after exercise training on land. *The Journal of Experimental Biology*, 222, jeb.213348. <https://doi.org/10.1242/jeb.213348>
- Metscher, B. D. (2009). MicroCT for comparative morphology: Simple staining methods allow high-contrast 3D imaging of diverse non-mineralized animal tissues. *BMC Physiology*, 9(1), 11. <https://doi.org/10.1186/1472-6793-9-11>
- Münkemüller, T., Lavergne, S., Bzeznik, B., Dray, S., Jombart, T., Schiffrers, K., & Thuiller, W. (2012). How to measure and test phylogenetic signal. *Methods in Ecology and Evolution*, 3(4), 743–756. <https://doi.org/10.1111/j.2041-210X.2012.00196.x>
- Nelson, J., Grande, T., & Wilson, M. (2016). *Fishes of the world*, Hoboken, NJ: John Wiley & Sons.
- Pace, C. M., & Gibb, A. C. (2009). Mudskipper pectoral fin kinematics in aquatic and terrestrial environments. *The Journal of Experimental Biology*, 212(Pt 14), 2279–2286. <https://doi.org/10.1242/jeb.029041>
- Pigliucci, M., Murren, C. J., & Schlichting, C. D. (2006). Phenotypic plasticity and evolution by genetic assimilation. *Journal of Experimental Biology*, 209(12), 2362–2367. <https://doi.org/10.1242/jeb.02070>
- Randall, Z. S., & Page, L. M. (2015). On the paraphyly of *Homaloptera* (Teleostei: Balitoridae) and description of a new genus of hillstream loaches from the Western Ghats of India. *Zootaxa*, 3926(1), 57–86. <https://doi.org/10.11646/zootaxa.3926.1.2>
- Ripley, B., & Venables, W. (2002). *Modern applied statistics with S* (4th ed.). New York: Springer.
- Sanford, G. M., Lutterschmidt, W. I., & Hutchison, V. H. (2002). The comparative method revisited. *Bioscience*, 52(9), 830–836. [https://doi.org/10.1641/0006-3568\(2002\)052\[0830:tcmr\]2.0.co;2](https://doi.org/10.1641/0006-3568(2002)052[0830:tcmr]2.0.co;2)
- Sawada, Y. (1982). Phylogeny and zoogeography of the superfamily Cobitoidea (Cyprinoidei, Cypriniformes). *Memoirs of the Faculty of Fisheries Hokkaido University*, 28(2), 65–223.
- Saxena, S. C., & Chandy, M. (1966). The pelvic girdle and fin in certain Indian hill stream fishes. *Journal of Zoology*, 148(2), 167–190. <https://doi.org/10.1111/j.1469-7998.1966.tb02946.x>
- Schindelin, J., Arganda-Carreras, I., Frise, E., Kaynig, V., Longair, M., Pietzsch, T., ... Cardona, A. (2012, July). Fiji: An open-source platform for biological-image analysis. *Nature Methods*, 9, 676–682. <https://doi.org/10.1038/nmeth.2019>
- Šlechtová, V., Bohlen, J., & Tan, H. H. (2007). Families of Cobitoidea (Teleostei; Cypriniformes) as revealed from nuclear genetic data and the position of the mysterious genera *Barbucca*, *Psilorhynchus*, *Serpenticobitis* and *Vaillantella*. *Molecular Phylogenetics and Evolution*, 44(3), 1358–1365. <https://doi.org/10.1016/j.ympev.2007.02.019>
- Stamatakis, A. (2014). RAxML version 8: A tool for phylogenetic analysis and post-analysis of large phylogenies. *Bioinformatics*, 30(9), 1312–1313. <https://doi.org/10.1093/bioinformatics/btu033>
- Standen, E. M., Du, T. Y., & Larsson, H. C. E. (2014). Developmental plasticity and the origin of tetrapods. *Nature*, 513(7516), 54–58. <https://doi.org/10.1038/nature13708>
- Stiassny, M. L. J., & Moore, J. A. (1992). A review of the pelvic girdle of acanthomorph fishes, with comments on hypotheses of acanthomorph intrarelationships. *Zoological Journal of the Linnean Society*, 104(3), 209–242. <https://doi.org/10.1111/j.1096-3642.1992.tb00923.x>
- Swofford, D. (2002). *Phylogenetic analysis using parsimony (and other methods)*. Sunderland, MA: Sinauer Associates.
- Tagliacollo, V. A., & Lanfear, R. (2018). Estimating improved partitioning schemes for ultraconserved elements. *Molecular Biology and Evolution*, 35(7), 1798–1811. <https://doi.org/10.1093/molbev/msy069>
- Tan, M., & Armbruster, J. W. (2018). Phylogenetic classification of extant genera of fishes of the order Cypriniformes (Teleostei: Ostariophysi). *Zootaxa*, 4476(1), 6–39. <https://doi.org/10.11646/zootaxa.4476.1.4>
- Trajano, E., Mugue, N., Krejca, J., Vidhayanon, C., Smart, D., & Borowsky, R. (2002). Habitat, distribution, ecology and behavior of cave balitorids from Thailand (Teleostei: Cypriniformes). *Ichthyological Exploration of Freshwaters*, 13(2), 169–184.
- West-Eberhard, M. J. (1989). Phenotypic plasticity and the origins of diversity. *Annual Review of Ecology and Systematics*, 20, 249–278. <https://doi.org/10.1146/annurev.es.20.110189.001341>
- Winterbottom, R. (1973). A descriptive synonymy of the striated muscles of the Teleostei. *Proceedings of the Academy of Natural Sciences of Philadelphia*, 125(125), 225–317.
- Wright, P. A., & Turko, A. J. (2016). Amphibious fishes: Evolution and phenotypic plasticity. *The Journal of Experimental Biology*, 219(15), 2245–2259. <https://doi.org/10.1242/jeb.126649>
- Yamanoue, Y., Setiamarga, D. H. E., & Matsuura, K. (2010). Pelvic fins in teleosts: Structure, function and evolution. *Journal of Fish Biology*, 77(6), 1173–1208. <https://doi.org/10.1111/j.1095-8649.2010.02674.x>

SUPPORTING INFORMATION

Additional supporting information may be found online in the Supporting Information section at the end of this article.

How to cite this article: Crawford CH, Randall ZS, Hart PB, et al. Skeletal and muscular pelvic morphology of hillstream loaches (Cypriniformes: Balitoridae). *Journal of Morphology*. 2020;1–16. <https://doi.org/10.1002/jmor.21247>